



Published in final edited form as:

J Bone Miner Res. 2012 February ; 27(2): 309–318. doi:10.1002/jbmr.541.

Adverse Effects of Hyperlipidemia on Bone Regeneration and Strength

F Pirih¹, J Lu², F Ye³, O Bezouglaia¹, E Atti¹, MG Ascenzi⁴, S Tetradis¹, LL Demer^{2,3,5,6}, T Aghaloo^{1,6}, and Y Tintut^{3,6}

F Pirih: fpirih@dentistry.ucla.edu; J Lu: jinxiulu@mednet.ucla.edu; F Ye: f.ye@ucla.edu; O Bezouglaia: obezouglaia@dentistry.ucla.edu; E Atti: eatti@dentistry.ucla.edu; MG Ascenzi: mgascenzi@mednet.ucla.edu; S Tetradis: stetradis@dentistry.ucla.edu; LL Demer: ldemer@mednet.ucla.edu; T Aghaloo: taghaloo@dentistry.ucla.edu; Y Tintut: ytintut@mednet.ucla.edu

¹Division of Diagnostic and Surgical Sciences, School of Dentistry, University of California, Los Angeles

²Department of Physiology, University of California, Los Angeles

³Division of Cardiology, Department of Medicine, University of California, Los Angeles

⁴Department of Orthopedic Surgery, University of California, Los Angeles

⁵Department of Bioengineering, University of California, Los Angeles

Abstract

Hyperlipidemia increases the risk for generation of lipid oxidation products, which accumulate in the subendothelial spaces of vasculature and bone. Atherogenic high-fat diets increase serum levels of oxidized lipids, which are known to attenuate osteogenesis in culture and to promote bone loss in mice. In this study, we investigated whether oxidized lipids affect bone regeneration and mechanical strength. Wild type and hyperlipidemic (*Ldlr*^{-/-}) mice were placed on a high-fat (HF) diet for 13 weeks. Bilateral cranial defects were introduced on each side of the sagittal suture, and 5 weeks post-surgery on the respective diets, the repair/regeneration of cranial bones and mechanical properties of femoral bones were assessed. MicroCT and histological analyses demonstrated that bone regeneration was significantly impaired by the HF diet in WT and *Ldlr*^{-/-} mice. In femoral bone, cortical bone volume fraction (BV/TV) was significantly reduced while cortical porosity was increased by the HF diet in *Ldlr*^{-/-} but not in WT mice. Femoral bone strength and stiffness, measured by three-point bending analysis, were significantly reduced by the HF diet in *Ldlr*^{-/-}, but not in WT mice. Serum analysis showed that the HF diet significantly increased levels of parathyroid hormone, TNF-alpha, calcium and phosphorus, whereas it reduced procollagen type I N-terminal propeptide, a serum marker of bone formation, in *Ldlr*^{-/-}, but not in WT mice. The serum level of carboxyl-terminal collagen crosslinks, a marker for bone resorption, was also 1.7-fold greater in *Ldlr*^{-/-} mice. These findings suggest that hyperlipidemia induces secondary hyperparathyroidism and impairs bone regeneration and mechanical strength.

Address all correspondence to: Yin Tintut, Ph.D., Division of Cardiology, David Geffen School of Medicine, University of California, Los Angeles, Center for the Health Sciences A2-237, 10833 Le Conte Ave, Los Angeles, CA. 90095-1679, Phone: (310) 206-9964, fax: (310) 825-4963, ytintut@mednet.ucla.edu.

⁶Senior Coauthors

Disclosure - Dr. Ascenzi is the inventor under granted and pending published patent applications related to her bone micro-structural research, the rights to which are licensed to Micro-Generated Algorithms, LLC, a California limited liability company in which she holds an interest. All other authors have no disclosure.

Keywords

Hyperlipidemia; parathyroid hormone; regeneration; osteoporosis

INTRODUCTION

Cardiovascular disease and osteoporosis are the two major causes of increased morbidity and mortality affecting the aging population. Hyperlipidemia, due to dietary intake or genetic mutations in cholesterol uptake and clearance, such as in low-density lipoprotein (LDL) receptor deficiency, has adverse effects on the vasculature, including development of atherosclerosis and vascular calcification. Under hyperlipidemic conditions, LDL particles pass through the endothelial barrier into the subendothelial space, where they are entrapped and oxidatively modified by reactive oxygen species produced by metabolically active, neighboring smooth muscle cells and macrophages (1). A similar process appears to occur in human osteoporotic bone, with oxidized lipoprotein particles accumulating in the perivascular subendothelial spaces (2). Osteoblasts also have the capacity to oxidatively modify lipoproteins (3), and products of lipid oxidation are detected in the marrow of hyperlipidemic mice (2,3).

The National Health and Nutrition Examination Survey (NHANES III) reports that 63% of osteoporotic patients have hyperlipidemia (4). Epidemiological studies reveal an inverse relationship between serum cholesterol levels and bone mineral content and density (5–9), independent of age and body mass index (10). Diet-induced hyperlipidemia is also associated with a reduction in bone mineral content and density in both mice and canines (11–13). Individuals with mutations in low-density lipoprotein receptor-related protein 5 (LRP5) have low bone mineral density and multiple spinal fractures (14).

Atherogenic high-fat diets further increase lipoprotein levels and their oxidative products (15,16). Importantly, regardless of whether due to a genetic or dietary abnormality, excessive lipid oxidation products attenuate osteogenic differentiation *in vitro* (17–19). In addition, oxidized lipids induce osteoclastogenesis and attenuate parathyroid hormone (PTH) and BMP-2 signaling (2,20–22). In mice, hyperlipidemia induces bone loss (11,12) and impairs anabolic effects of intermittent parathyroid hormone (PTH)(23,24), a regimen now used for clinical treatment of women with postmenopausal osteoporosis. Using ApoA-I mimetic peptides, we recently demonstrated that hyperlipidemia-induced PTH resistance in mice was mediated by oxidized lipids (24). However, the effects of hyperlipidemia on the functional parameters of bone are not known. In the present study, we tested the effects of hyperlipidemia on bone repair, regeneration and mechanical strength in mice.

METHODS

Animals

Ldlr^{-/-} and wild type (C57BL/6) mice were obtained from the Jackson Laboratory (Bar Harbor, ME). All the experimental protocols were reviewed and approved by the Institutional Animal Care and Use Committee of the University of California at Los Angeles. Seven week-old male BL6 (WT) and *Ldlr*^{-/-} (The Jackson Laboratory) mice (n = 6/group) were placed on chow or an atherogenic (Paigen) diet (HF diet; 20.5% kcal from protein, 42.4% kcal from carbohydrate, 37.1% kcal from fat, formulated in pellets, TD 90221, Harlan Teklad) for 13 weeks. This diet increased lipid oxidation levels (11,24). Bone regeneration was assayed by a cranial defect model (25,26). After 13 weeks on the diet, two 3-mm defects were created on each side of the sagittal suture under anesthesia with a trephine burr and copious saline irrigation, without trauma to the underlying dura. The

incision was closed, and the animals were closely monitored for wound healing while receiving the respective diet. Five weeks post surgery, the mice were euthanized, and blood and tissues were procured.

MicroCT analysis

Cranial bones were carefully harvested, fixed in 4% paraformaldehyde and stored in 70% ethanol until they were scanned with μ CT (Skyscan 1172, Aartselaar, Belgium). An isotropic voxel size of 15 μ m, at 55 kVp, 167 μ A and 0.5 mm aluminum filter were used. Axial slices (1024 \times 1024) were reconstructed, and analysis was performed using the Skyscan software. The architectural parameters evaluated were tissue volume (TV), bone volume (BV), bone volume fraction (BV/TV), and bone mineral density (BMD). TV was set as the volume of the original bone defect of a cylinder with a 3 mm diameter. BV then represents the volume of the mineralized tissue formed within the defect during healing.

Right femoral bones were harvested and analyzed for bone volume fraction (BV/TV), cortical porosity, and bone mineral density by μ CT (Skyscan 1172, Aartselaar, Belgium). The data were collected at 55 kVp and 72 μ A at a resolution of 12 μ m. Volumetric analysis was performed using Skyscan software. For cortical analysis at mid-diaphysis, the length of each femoral bone was measured, and 40 mid-diaphyseal slices were used. After performing microCT, the femurs were subjected to a three-point bending test.

Three-point bending test

The mechanical properties of femoral bones were tested by three-point bending tests at the Kureha Special Laboratory Co., Ltd (Tokyo, Japan) using established protocols for mouse bones (27). The span between the two supports of the femur was set at 6 mm; the upper loading device was aligned to the midshaft; and load was applied at a constant displacement rate of 6 mm/min to total failure. Maximum load at failure (N), stiffness (N/mm) and energy to failure (N.mm) were determined.

Trabecular Bone histomorphometric analysis

The left femurs were subjected to static and dynamic histomorphometry at the UCLA Bone Histomorphometric Laboratory, as previously described (23). Briefly, bones were fixed in 70% ethanol, dehydrated, embedded undecalcified in methyl methacrylate, longitudinal sections (5 μ m thick) cut with a microtome (Microm, Richards-Allan Scientific, Kalamazoo, MI) and stained with toluidine blue, pH 6.4. For dynamic histomorphometry, including mineralizing surface per bone surface and bone formation rate, calcein and demeclocycline injections were performed 10 and 2 days prior to harvest; unstained sections were embedded in methylmethacrylate and examined by fluorescence microscopy. Mineralizing surface was assessed by calcein-labeled surface length relative to total surface length, and bone formation rate was calculated based on the separation of the dual fluorescence labeling. Bone formation and resorption were measured in a defined area between 181 μ m and 725 μ m below the growth plate, using the OsteoMeasure morphometry system (Osteometrics, Atlanta, GA). The terminology and units used are those recommended by the Histomorphometry Nomenclature Committee of the American Society for Bone and Mineral Research.

Serum biochemical assays

The serum was pooled and assayed in quadruplicate. Serum levels of iPTH (Immunotopics), procollagen type I N-terminal propeptide (PINP; Immunodiagnostic Systems), carboxyl-terminal collagen crosslinks (CTX, RATLAPS; Immunodiagnostic Systems), RANKL (R&D Systems) and OPG (R&D Systems) were measured following the manufacturers'

protocols. Serum levels of lipids and glucose were performed by the UCLA Atherosclerosis Research Unit Core Laboratory. Serum calcium levels were assayed using the *o*-cresolphthalein complexone method (Advanced Bioscreen). Serum phosphate levels were performed by the Diagnostic Laboratory of the UCLA Division of Laboratory Animal Medicine.

Realtime RT-qPCR

Total RNA was isolated from the calvaria and humeri (6/group). Real-time RT-qPCR was performed using the One-Step RT-qPCR SuperMix Kit (BioChain, Inc.) and Mx3005P Real-Time PCR System (Stratagene) (20,28,29).

Histological analysis

Cranial bones from the first four mice of each group were decalcified, embedded in paraffin, sectioned at 5 μ m, and stained with hematoxylin and eosin, by the UCLA Translational Pathology Core Laboratory. Serial sections were immunostained with anti-CD11b (Abbiotec, LLC; CA), anti-osteopontin (Abcam, CA), and anti-calponin (SantaCruz Biotechnology, Inc., CA), and TRAP histochemical staining was performed, as described previously(2).

Statistical analysis

The effects of the HF diet was evaluated by comparing the chow vs. HF groups within each mouse strain (WT or *Ldlr*^{-/-}) using Student's *t*-test. Values were expressed as means \pm SEM. A value of $p \leq 0.05$ was considered statistically significant.

RESULTS

Effects of the HF diet on serum lipid levels

As shown in Table 1, total serum cholesterol was increased by 8-fold in *Ldlr*^{-/-} and 2-fold in WT mice in response to the HF diet, whereas HDL was reduced by 94% in *Ldlr*^{-/-} and 20% in WT mice. In addition, the HF diet increased serum glucose levels 1.7-fold in *Ldlr*^{-/-}, but not in WT mice, whereas the HF diet decreased triglyceride levels in both groups (Table 1).

Effects of the HF diet on bone regeneration

To test the effects of hyperlipidemia and the HF diet on bone regeneration, bilateral cranial defects were surgically introduced after 13 weeks on the diet. Five weeks after the defects were introduced, the calvaria were isolated and bone regeneration was assessed. MicroCT analysis showed that bone regeneration and partial healing of the defect occurred in WT and *Ldlr*^{-/-} mice on the chow diet (Figure 1A). Bone healing was greatly impaired by the HF diet in both groups of mice (Figure 1A). Both bone surface and bone volume were significantly reduced by the HF diet (Figure 1B). In agreement with the microCT observations, histological analysis (Figure 1C) of the demineralized cranial bones showed that fibrous tissue covered the entire defect in all the groups, and partial healing with bone occurred in some groups within the 5-week period. In the chow groups, the defects were covered with thick fibrous tissue and with lamellar bone formation at the periphery of the defect. In the HF groups, the defects were covered with thin, fibrous tissue and with little or no lamellar bone. To identify cell types, we used immunohistochemical staining for osteoblastic, myofibroblastic, and immune cells, using anti-osteopontin, calponin and CD11b antibodies, respectively. Regenerative fibrous tissue was immunopositive for osteopontin and calponin, consistent with osteoblastic and/or myofibroblastic cells. Granulation tissue was immunopositive for CD11b (Figure 1D). Osteoclastic cells,

identified by TRAP histochemical staining, were negative in the fibrous tissue, but positive in the adjacent calvarial bone (Figure 1D).

Effects of the HF diet on bone strength and microCT parameters

To test the effect of hyperlipidemia and the HF diet on mechanical strength, femoral bones were isolated and subjected to a three-point bending test. Results showed that both maximum load at failure and stiffness were significantly reduced by the HF diet only in *Ldlr*^{-/-} mice (Figure 2C) although the energy to failure was not significantly altered by the HF diet (data not shown). MicroCT analysis prior to the bending test revealed that cortical BV/TV was significantly reduced and cortical porosity was significantly increased by the HF diet in *Ldlr*^{-/-}, but not in WT mice (Figure 2A). Bone mineral density was reduced by the HF diet in both groups [WT: 1.49 ± 0.01 (Chow) vs. 1.46 ± 0.01 (HF), *p* < 0.01; *Ldlr*^{-/-}: 1.49 ± 0.01 (Chow) vs. 1.46 ± 0.02 g/cm³ (HF), *p* < 0.01].

To determine whether inhibition of oxidized lipids reverses the effects of HF diet, we analyzed unpublished data from bone samples from previous experiments (24) in which mice were treated with the ApoA-I mimetic peptide, D-4F, a known inhibitor of oxidized lipids in vivo. Three treatment groups of *Ldlr*^{-/-} mice were analyzed: (1) 13 weeks of chow diet, (2) 13 weeks of HF diet, and (3) 6-weeks of HF diet followed by 7 weeks of cotreatment with HF diet and D-4F. Results showed that D-4F blunted the effects of the HF diet on cortical BV/TV and cortical porosity, suggesting that the adverse effects of hyperlipidemia were mediated by oxidized lipids (Figure 2B). As shown in Figure 2D, BV/TV correlated with maximum load at failure, a measure of strength (*r* = 0.69), whereas cortical porosity correlated inversely with stiffness (*r* = -0.74).

Histomorphometric analysis (Table 2) of femoral trabecular bone showed that BV/TV was significantly reduced by the HF diet in *Ldlr*^{-/-} mice, and a trend toward reduction (*p* = 0.08) was observed in WT mice. Trabecular bone area and thickness were significantly reduced by the HF diet in both groups. Interestingly, trabecular BFR/BS was significantly increased by the HF diet in the WT group but not in the *Ldlr*^{-/-} group. Consequently, mineralizing surface area (MS/BS) was also increased, but only in the WT group. Other parameters, Ob.S/BS, Oc.S/BS, N.Ob/T.Ar and N.Oc/T.Ar, were not altered by the HF diet in either group, suggesting that the changes in trabecular bone area, thickness, and formation rate are mediated by function, rather than density, of osteoblastic and osteoresorptive cells.

Effects of the HF diet on serum bone markers

Serum analysis for bone-related markers showed that the HF diet significantly elevated the levels of iPTH and TNF-α in *Ldlr*^{-/-} but not in WT mice (Figure 3A). The HF diet also significantly reduced the bone formation marker, PINP, only in *Ldlr*^{-/-}, and the HF diet induced a 1.7-fold increase in levels of the resorption marker, CTX, in *Ldlr*^{-/-} mice (40% vs. 23%) (Figure 3B). Similarly, the HF diet increased serum calcium levels by 2.1-fold in *Ldlr*^{-/-} mice, but by only 1.4-fold in WT mice (Figure 3C). The HF diet also increased serum phosphorus levels by 1.5-fold in *Ldlr*^{-/-} mice (Figure 3D). Interestingly, the HF diet upregulated serum IGF-1 levels in WT but not in *Ldlr*^{-/-} mice (Figure 3A). Paradoxically, the HF-fed mice had lower serum RANKL and higher OPG levels than chow-fed mice (Table III).

Effects of the HF diet on gene expression

To assess the effects of the HF diet on osteogenic regulatory gene expression, we performed realtime RT-qPCR of RNA isolated from humeri. As shown in Figure 4A, expression of PTH receptor (PTH1R) and IGF-1 was downregulated in *Ldlr*^{-/-} but not in the WT group. In contrast, expression of sclerostin (Sost), a glycoprotein secreted by osteocytes, was

significantly downregulated by the HF diet in WT group but not *Ldlr*^{-/-} group (Figure 4B). The expression of the master regulator of mature osteoblasts, *Cbfa1* (*Runx2*), was downregulated in both strains (Figure 4B). The osteoclast regulatory factor, RANKL, was upregulated only in WT, whereas it was downregulated in *Ldlr*^{-/-} mice, and OPG expression was not altered (Figure 4C). Oil red O staining of tibial bones revealed that lipids were increasingly accumulated in the bone marrow of the HF diet-fed WT and *Ldlr*^{-/-} mice (Figure 5).

DISCUSSION

The present study supports the findings of diet-induced osteoporotic changes in hyperlipidemic mice (11,12,30). Recently, we demonstrated that lipid oxidation products mediate the adverse effects of high fat diets on bone (24). In this report, we extend our findings to demonstrate that oxidized lipids and/or hyperlipidemia also adversely affect bone mechanical strength and impair bone regeneration. The present findings indicate that cortical bone volume and cortical porosity are blunted by treatment with the HDL mimetic peptide, D-4F, further supporting the concept that the adverse effects of the HF diet are mediated by lipid oxidation products. More than one mechanism may account for the adverse effects on bone regeneration and mechanical function. We have previously shown that oxidized lipids inhibit differentiation of osteoblasts (12). Hirasawa et al showed that the HF diet also increases osteoblast apoptosis (11). Increased osteoclastic resorption, evidenced by increased levels of CTX in *Ldlr*^{-/-} mice, may also contribute to bone loss. Interestingly, it appears that the HF diet induces bone turnover in WT but not in *Ldlr*^{-/-} mice.

Notably, in *Ldlr*^{-/-} mice the HF diet is not only atherogenic, it is also diabetogenic, as evidenced by increased serum glucose levels. The high levels of serum glucose observed in the HF diet-treated *Ldlr*^{-/-} mice suggest some degree of insulin resistance, as previously described with the Western diet (31). Given the known relationship between diabetic hyperglycemia and oxidant stress (32), hyperglycemia may contribute, in part, to the observed effects on bone, at the level of either enhancing lipid oxidation and/or inducing inflammatory cytokines, such as via advanced glycation endproducts (33). The HF diet-induced serum glucose levels were not affected by the D-4F treatment (data not shown). This is consistent with the findings by Morgantini and colleagues, who found that D-4F did not affect serum glucose levels in streptozotocin-treated *ApoE*^{-/-} mice (34).

We also demonstrate that, the HF diet also induces hyperparathyroidism in these mice, as evidenced by the increased serum levels of intact PTH, calcium, and phosphorus. The non-physiological calcium measurement in the HF-fed *Ldlr*^{-/-} mice may be pseudohypercalcemia due to the turbidity of lipemic serum (35). The potential mechanisms of secondary hyperparathyroidism include renal PTH-resistance leading to phosphate retention or a change in the set-point of the calcium-sensing receptor. Interestingly, PTH receptor expression was downregulated in humeri of these mice. This effect may be a negative feedback response to increased PTH levels, since PTH reduces expression of its receptor (36). Alternatively, the PTH receptor downregulation could be due to direct effects of oxidized lipids on osteoblasts, as we have shown previously (20).

Interestingly, the present results showed that hyperlipidemia differentially affects cranial, cortical, and trabecular bone. Cranial regeneration was inhibited in both WT and *Ldlr*^{-/-} mice. In cortical bone, the HF diet had adverse effects mainly on *Ldlr*^{-/-} mice. In trabecular bone, the HF diet increased bone formation rate in the WT but not the *Ldlr*^{-/-} group. The latter effect may be in response to increased levels of serum IGF-1, which is observed only in WT mice, consistent with the findings of Elis et al. that serum IGF-1 promotes post-natal

bone growth (37). The differences in responsiveness of trabecular and cortical bone may also be due to their known metabolic differences.

Paradoxically, HF-fed mice had lower serum RANKL and higher serum OPG levels than chow-fed mice (Table III), consistent with the changes in mRNA expression in bone tissue. Interestingly, the same trend is seen in patients with coronary atherosclerosis: lower serum RANKL and higher serum OPG levels (38,39). One possibility is that the observed increases in serum calcium, phosphate, and CTX in the HF-fed *Ldlr*^{-/-} mice may be due to non-canonical pathways of osteoclastogenesis, such as through TNF- α and IGF-I (40).

Gene expression patterns revealed effects of the HF diet on factors affecting both osteoprogenitors and maturing osteoblasts. Expression of *Sost*, which affects osteoprogenitors (41) via Wnt inhibition (42), was downregulated by the HF diet in WT mice, suggesting that hyperlipidemia, or resulting inflammation, may affect osteocytes. Concurrently, *Cbfa1* (*Runx2*), the master regulator of differentiation of mature osteoblasts, was downregulated by the HF diet, suggesting that the diet may increase osteoprogenitor cells but reduce differentiation of osteoblasts. Osteoporotic bone marrow contains fewer osteogenic cells but more adipocytic cells (43). One possible mechanism is induction of adipogenic differentiation by oxidized lipids in cultured bone marrow stromal cells *in vitro* (44). Our current findings show that bone marrow of high fat diet-fed *Ldlr*^{-/-} mice has more adipocytes than control bone marrow, suggesting that oxidized lipids direct marrow stromal cells toward an adipogenic lineage.

It is notable that the HF diet formulation implemented in this study (“Paigen atherogenic” diet) contains 0.5% cholate, a cholesterol-derived bile salt. Many other HF diet formulations for mice, such as the ‘Western diet,’ are not supplemented with cholate. The Western HF diet promotes insulin resistance (45) and hypertriglyceridemia (46) as well as hypercholesterolemia, all contributing to an atherosclerotic phenotype resembling that seen in human metabolic syndrome. In contrast, cholate enhances intestinal fat absorption, promotes inflammation and fibrosis, and accentuates hypercholesterolemia by feedback inhibition of cholesterol-7- α -hydroxylase (*CYP7A1*), all contributing to an advanced atherosclerotic phenotype (more sclerotic than atheromatous). On the Paigen atherogenic diet, *PDZK1/Apoe* DKO mice even develop arterial occlusion (47), and *Ldlr*^{-/-} mice, skin xanthomata (48), closely resembling advanced human hyperlipidemia-induced atherosclerotic disease.

Overall, these findings support the hypothesis that hyperlipidemia adversely affects bone regeneration and functional parameters through actions of oxidized lipids. We speculate that oxidized lipids may have an even broader role in redirecting lineage commitment of stem cells in general.

Acknowledgments

This research was supported by funding from National Institute of Health (DK081346, DK081346-S1, HL081202 and DE019465).

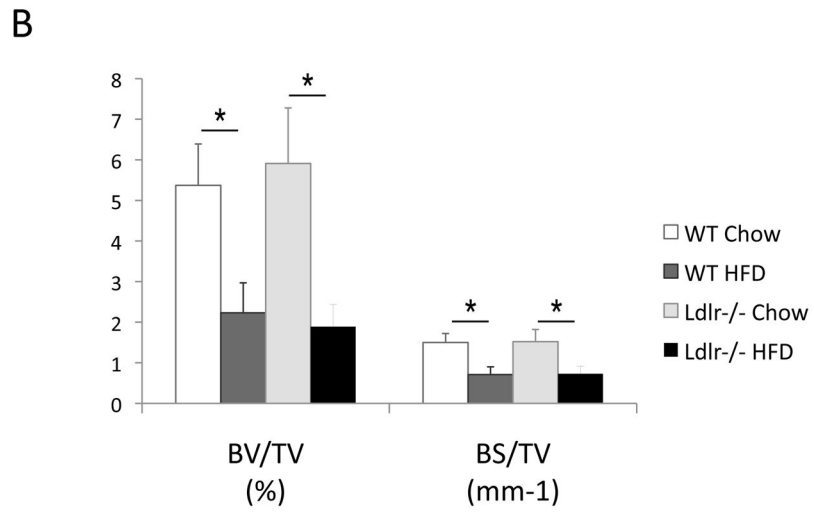
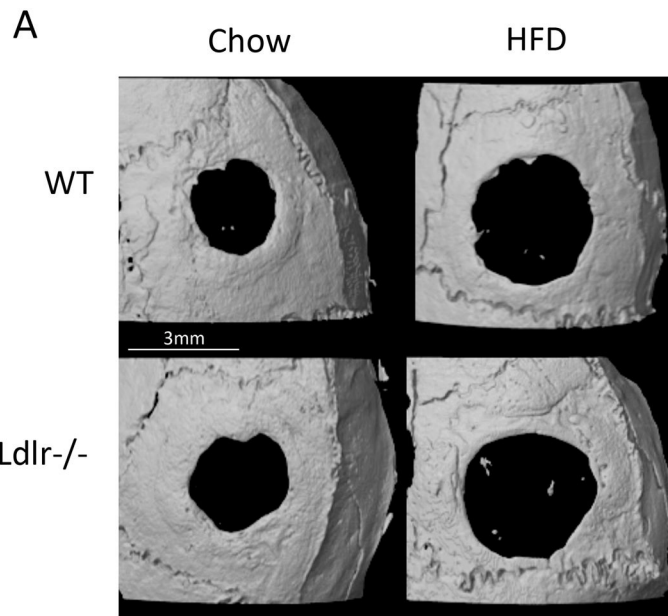
References

1. Navab M, Berliner JA, Watson AD, Hama SY, Territo MC, Lusis AJ, Shih DM, Van Lenten BJ, Frank JS, Demer LL, Edwards PA, Fogelman AM. The Yin and Yang of oxidation in the development of the fatty streak. A review based on the 1994 George Lyman Duff Memorial Lecture. *Arterioscler Thromb Vasc Biol.* 1996; 16(7):831–842. [PubMed: 8673557]
2. Tintut Y, Morony S, Demer LL. Hyperlipidemia promotes osteoclastic potential of bone marrow cells *ex vivo*. *Arterioscler Thromb Vasc Biol.* 2004; 24(2):e6–10. [PubMed: 14670933]

3. Brodeur MR, Brissette L, Falstraull L, Ouellet P, Moreau R. Influence of oxidized low-density lipoproteins (LDL) on the viability of osteoblastic cells. *Free Radic Biol Med*. 2008; 44 (4):506–517. [PubMed: 18241787]
4. Bilezikian, JP.; Davidson, M.; Hendrix, S.; Liu, L.; Louie, M. Co-Morbidity of Decreased Bone Mineral Density (BMD) and Increased Cholesterol Levels among Women Aged 65 Years and Older: Results from NHANES III. *ASBMR 27th Annual Meeting*:SU130; 2005.
5. Cui LH, Shin MH, Chung EK, Lee YH, Kweon SS, Park KS, Choi JS. Association between bone mineral densities and serum lipid profiles of pre- and post-menopausal rural women in South Korea. *Osteoporos Int*. 2005; 16(12):1975–1981. [PubMed: 16167087]
6. Hsu YH, Venners SA, Terwedow HA, Feng Y, Niu T, Li Z, Laird N, Brain JD, Cummings SR, Bouxsein ML, Rosen CJ, Xu X. Relation of body composition, fat mass, and serum lipids to osteoporotic fractures and bone mineral density in Chinese men and women. *Am J Clin Nutr*. 2006; 83(1):146–154. [PubMed: 16400063]
7. Nuzzo V, de Milita AM, Ferraro T, Monaco A, Florio E, Miano P, Montemarano E, Zuccoli A, de Terlizzi F. Analysis of skeletal status by quantitative ultrasonometry in a cohort of postmenopausal women with high blood cholesterol without documented osteoporosis. *Ultrasound Med Biol*. 2009; 35(5):717–722. [PubMed: 19251356]
8. Tanko LB, Bagger YZ, Christiansen C. Low bone mineral density in the hip as a marker of advanced atherosclerosis in elderly women. *Calcif Tissue Int*. 2003; 73(1):15–20. [PubMed: 14506949]
9. Wu S, De Luca F. Role of cholesterol in the regulation of growth plate chondrogenesis and longitudinal bone growth. *J Biol Chem*. 2004; 279(6):4642–4647. [PubMed: 14612457]
10. Lekamwasam S, Weerathna T, Rodrigo M, Arachchi WK, Munidasa D. Osteoporosis and cardiovascular risk among premenopausal women in Sri Lanka. *J Clin Densitom*. 2009; 12(2): 245–250. [PubMed: 19328732]
11. Hirasawa H, Tanaka S, Sakai A, Tsutsui M, Shimokawa H, Miyata H, Moriwaki S, Niida S, Ito M, Nakamura T. ApoE gene deficiency enhances the reduction of bone formation induced by a high-fat diet through the stimulation of p53-mediated apoptosis in osteoblastic cells. *J Bone Miner Res*. 2007; 22(7):1020–1030. [PubMed: 17388726]
12. Parhami F, Tintut Y, Beamer WG, Gharavi N, Goodman W, Demer LL. Atherogenic high-fat diet reduces bone mineralization in mice. *J Bone Miner Res*. 2001; 16(1):182–188. [PubMed: 11149483]
13. Turek JJ, Watkins BA, Schoenlein IA, Allen KG, Hayek MG, Aldrich CG. Oxidized lipid depresses canine growth, immune function, and bone formation. *J Nutr Biochem*. 2003; 14 (1):24–31. [PubMed: 12559474]
14. Saarinen A, Saukkonen T, Kivela T, Lahtinen U, Laine C, Somer M, Toiviainen-Salo S, Cole WG, Lehesjoki AE, Makitie O. Low density lipoprotein receptor-related protein 5 (LRP5) mutations and osteoporosis, impaired glucose metabolism and hypercholesterolaemia. *Clin Endocrinol (Oxf)*. 72(4):481–488. [PubMed: 19673927]
15. Laurila A, Cole SP, Merat S, Obonyo M, Palinski W, Fierer J, Witztum JL. High-fat, high-cholesterol diet increases the incidence of gastritis in LDL receptor-negative mice. *Arterioscler Thromb Vasc Biol*. 2001; 21(6):991–996. [PubMed: 11397709]
16. Navab M, Hama SY, Cooke CJ, Anantharamaiah GM, Chaddha M, Jin L, Subbanagounder G, Faull KF, Reddy ST, Miller NE, Fogelman AM. Normal high density lipoprotein inhibits three steps in the formation of mildly oxidized low density lipoprotein: step 1. *J Lipid Res*. 2000; 41(9): 1481–1494. [PubMed: 10974056]
17. Almeida M, Ambrogini E, Han L, Manolagas SC, Jilka RL. Increased lipid oxidation causes oxidative stress, increased peroxisome proliferator-activated receptor-gamma expression, and diminished pro-osteogenic Wnt signaling in the skeleton. *J Biol Chem*. 2009; 284(40):27438–27448. [PubMed: 19657144]
18. Mody N, Parhami F, Sarafian TA, Demer LL. Oxidative stress modulates osteoblastic differentiation of vascular and bone cells. *Free Radic Biol Med*. 2001; 31(4):509–519. [PubMed: 11498284]

19. Parhami F, Morrow AD, Balucan J, Leitinger N, Watson AD, Tintut Y, Berliner JA, Demer LL. Lipid oxidation products have opposite effects on calcifying vascular cell and bone cell differentiation. A possible explanation for the paradox of arterial calcification in osteoporotic patients. *Arterioscler Thromb Vasc Biol.* 1997; 17(4):680–687. [PubMed: 9108780]
20. Huang MS, Morony S, Lu J, Zhang Z, Bezouglaia O, Tseng W, Tetradis S, Demer LL, Tintut Y. Atherogenic phospholipids attenuate osteogenic signaling by BMP-2 and parathyroid hormone in osteoblasts. *J Biol Chem.* 2007; 282(29):21237–21243. [PubMed: 17522049]
21. Parhami F, Fang ZT, Fogelman AM, Andalibi A, Territo MC, Berliner JA. Minimally modified low density lipoprotein-induced inflammatory responses in endothelial cells are mediated by cyclic adenosine monophosphate. *J Clin Invest.* 1993; 92(1):471–478. [PubMed: 8392092]
22. Tintut Y, Parhami F, Tsingotjidou A, Tetradis S, Territo M, Demer LL. 8-Isoprostaglandin E2 enhances receptor-activated NFkappa B ligand (RANKL)-dependent osteoclastic potential of marrow hematopoietic precursors via the cAMP pathway. *J Biol Chem.* 2002; 277(16):14221–14226. [PubMed: 11827970]
23. Huang MS, Lu J, Ivanov Y, Sage AP, Tseng W, Demer LL, Tintut Y. Hyperlipidemia impairs osteoanabolic effects of PTH. *J Bone Miner Res.* 2008; 23(10):1672–1679. [PubMed: 18505371]
24. Sage AP, Lu J, Atti E, Tetradis S, Ascenzi MG, Adams DJ, Demer LL, Tintut Y. Hyperlipidemia induces resistance to PTH bone anabolism in mice via oxidized lipids. *J Bone Miner Res.* 2011
25. Cowan CM, Shi YY, Aalami OO, Chou YF, Mari C, Thomas R, Quarto N, Contag CH, Wu B, Longaker MT. Adipose-derived adult stromal cells heal critical-size mouse calvarial defects. *Nat Biotechnol.* 2004; 22(5):560–567. [PubMed: 15077117]
26. Seo BM, Sonoyama W, Yamaza T, Coppe C, Kikuri T, Akiyama K, Lee JS, Shi S. SHED repair critical-size calvarial defects in mice. *Oral Dis.* 2008; 14(5):428–434. [PubMed: 18938268]
27. Bischoff DS, Sakamoto T, Ishida K, Makhijani NS, Gruber HE, Yamaguchi DT. CXC receptor knockout mice: characterization of skeletal features and membranous bone healing in the adult mouse. *Bone.* 48(2):267–274. [PubMed: 20870046]
28. Huang MS, Sage AP, Lu J, Demer LL, Tintut Y. Phosphate and pyrophosphate mediate PKA-induced vascular cell calcification. *Biochem Biophys Res Commun.* 2008; 374(3):553–558. [PubMed: 18655772]
29. Morony S, Tintut Y, Zhang Z, Cattley RC, Van G, Dwyer D, Stolina M, Kostenuik PJ, Demer LL. Osteoprotegerin inhibits vascular calcification without affecting atherosclerosis in *ldlr(-/-)* mice. *Circulation.* 2008; 117(3):411–420. [PubMed: 18172035]
30. Hjortnaes J, Butcher J, Figueiredo JL, Riccio M, Kohler RH, Kozloff KM, Weissleder R, Aikawa E. Arterial and aortic valve calcification inversely correlates with osteoporotic bone remodelling: a role for inflammation. *Eur Heart J.* 2010; 31(16):1975–1984. [PubMed: 20601388]
31. Towler DA, Bidder M, Latifi T, Coleman T, Semenkovich CF. Diet-induced diabetes activates anosteogenic gene regulatory program in the aortas of low density lipoprotein receptor-deficient mice. *J Biol Chem.* 1998; 273(46):30427–30434. [PubMed: 9804809]
32. Esposito K, Nappo F, Marfella R, Giugliano G, Giugliano F, Ciotola M, Quagliari L, Ceriello A, Giugliano D. Inflammatory cytokine concentrations are acutely increased by hyperglycemia in humans: role of oxidative stress. *Circulation.* 2002; 106(16):2067–2072. [PubMed: 12379575]
33. Yan SF, Ramasamy R, Naka Y, Schmidt AM. Glycation, inflammation, and RAGE: a scaffold for the macrovascular complications of diabetes and beyond. *Circ Res.* 2003; 93 (12):1159–1169. [PubMed: 14670831]
34. Morgantini C, Imaizumi S, Grijalva V, Navab M, Fogelman AM, Reddy ST. Apolipoprotein A-I mimetic peptides prevent atherosclerosis development and reduce plaque inflammation in a murine model of diabetes. *Diabetes.* 2010; 59(12):3223–3228. [PubMed: 20826564]
35. Kroll MH. Evaluating interference caused by lipemia. *Clin Chem.* 2004; 50(11):1968–1969. [PubMed: 15502078]
36. Koh AJ, Beecher CA, Rosol TJ, McCauley LK. 3',5'-Cyclic adenosine monophosphate activation in osteoblastic cells: effects on parathyroid hormone-1 receptors and osteoblastic differentiation in vitro. *Endocrinology.* 1999; 140(7):3154–3162. [PubMed: 10385409]

37. Elis S, Courtland HW, Wu Y, Fritton JC, Sun H, Rosen CJ, Yakar S. Elevated serum IGF-1 levels synergize PTH action on the skeleton only when the tissue IGF-1 axis is intact. *J Bone Miner Res.* 25(9):2051–2058. [PubMed: 20499370]
38. Schoppet M, Sattler AM, Schaefer JR, Herzum M, Maisch B, Hofbauer LC. Increased osteoprotegerin serum levels in men with coronary artery disease. *J Clin Endocrinol Metab.* 2003; 88(3):1024–1028. [PubMed: 12629080]
39. Schoppet M, Schaefer JR, Hofbauer LC. Low serum levels of soluble RANK ligand are associated with the presence of coronary artery disease in men. *Circulation.* 2003; 107(11):e76. author reply e76. [PubMed: 12654623]
40. Hemingway F, Taylor R, Knowles HJ, Athanasou NA. RANKL-independent human osteoclast formation with APRIL, BAFF, NGF, IGF I and IGF II. *Bone.* 48(4):938–944. [PubMed: 21193069]
41. Derfoul A, Carlberg AL, Tuan RS, Hall DJ. Differential regulation of osteogenic marker gene expression by Wnt-3a in embryonic mesenchymal multipotential progenitor cells. *Differentiation.* 2004; 72(5):209–223. [PubMed: 15270777]
42. Semenov M, Tamai K, He X. SOST is a ligand for LRP5/LRP6 and a Wnt signaling inhibitor. *J Biol Chem.* 2005; 280(29):26770–26775. [PubMed: 15908424]
43. Meunier P, Aaron J, Edouard C, Vignon G. Osteoporosis and the replacement of cell populations of the marrow by adipose tissue. A quantitative study of 84 iliac bone biopsies. *Clin Orthop Relat Res.* 1971; 80:147–154. [PubMed: 5133320]
44. Parhami F, Jackson SM, Tintut Y, Le V, Balucan JP, Territo M, Demer LL. Atherogenic diet and minimally oxidized low density lipoprotein inhibit osteogenic and promote adipogenic differentiation of marrow stromal cells. *J Bone Miner Res.* 1999; 14(12):2067–2078. [PubMed: 10620066]
45. Getz GS, Reardon CA. Diet and murine atherosclerosis. *Arterioscler Thromb Vasc Biol.* 2006; 26(2):242–249. [PubMed: 16373607]
46. Vergnes L, Phan J, Strauss M, Tafuri S, Reue K. Cholesterol and cholate components of an atherogenic diet induce distinct stages of hepatic inflammatory gene expression. *J Biol Chem.* 2003; 278(44):42774–42784. [PubMed: 12923166]
47. Yesilaltay A, Daniels K, Pal R, Krieger M, Kocher O. Loss of PDZK1 causes coronary artery occlusion and myocardial infarction in Paigen diet-fed apolipoprotein E deficient mice. *PLoS One.* 2009; 4(12):e8103. [PubMed: 19956623]
48. Ishibashi S, Goldstein JL, Brown MS, Herz J, Burns DK. Massive xanthomatosis and atherosclerosis in cholesterol-fed low density lipoprotein receptor-negative mice. *J Clin Invest.* 1994; 93(5):1885–1893. [PubMed: 8182121]



C

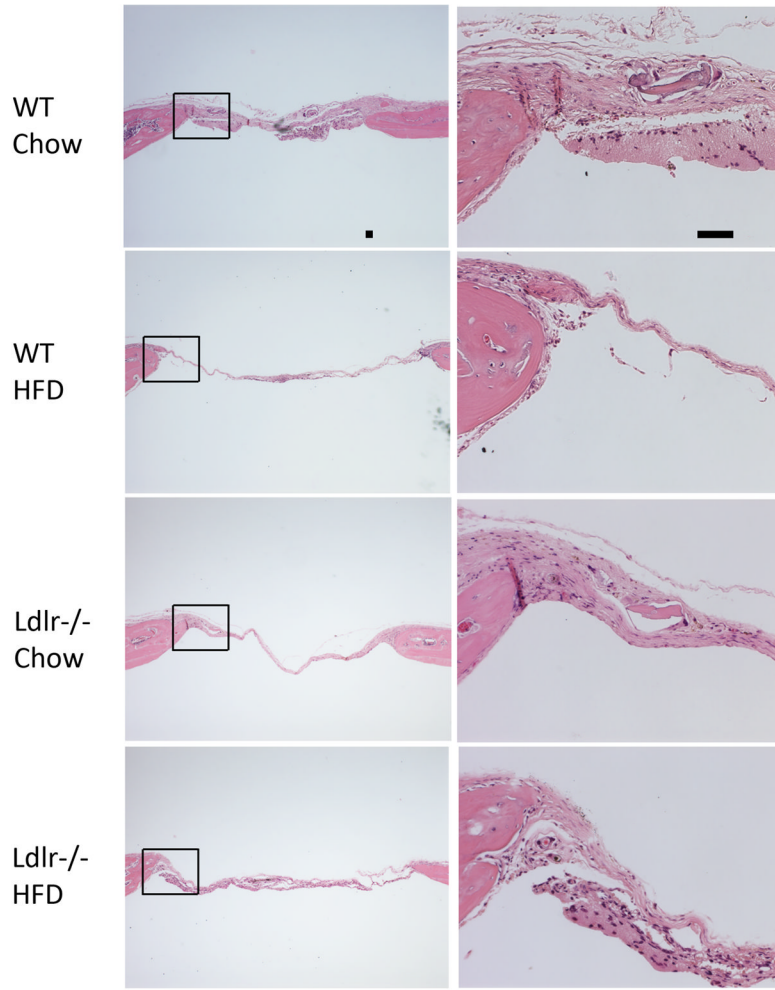


Figure 1D

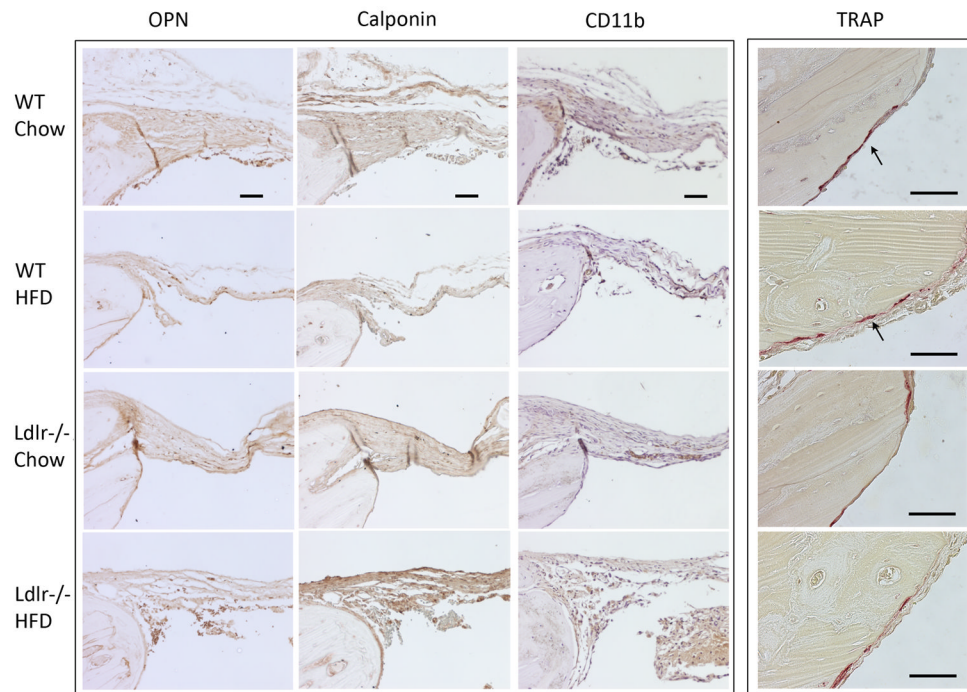
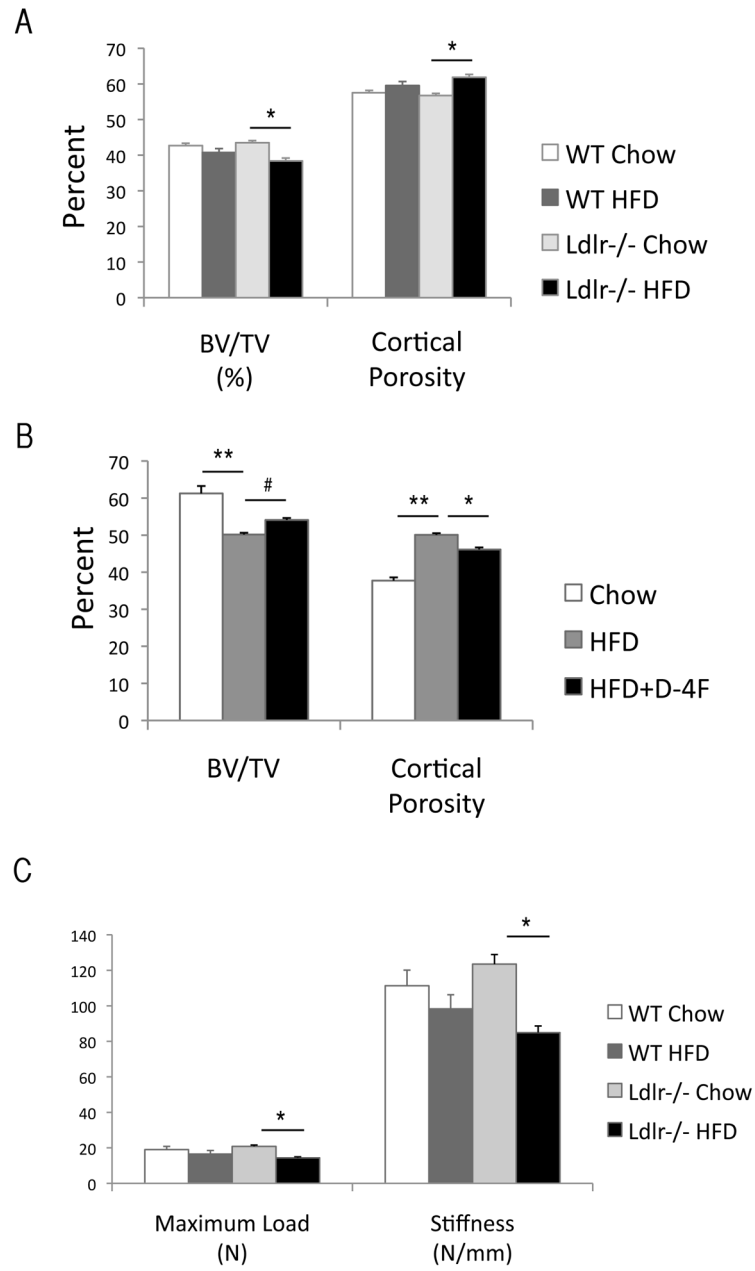


Figure 1. Effects of the HF diet on bone regeneration

(A) Three-dimensional microCT images of cranial defects in WT and *Ldlr*^{-/-} mice, with or without the HF diet (HFD). (B) MicroCT analysis of cranial bone volume (BV/TV) and surface (BS/TV). **p* < 0.05. (C) Hematoxylin and eosin analysis of cranial bones. Granulation tissue (arrows), which is distinguished from the regenerative fibrous material by its hypercellularity, lack of fibers, and lack of connection with the adjacent bone, was also present in some sections. (D) Immunohistochemical staining for osteopontin (OPN), calponin, CD11b and histochemical staining for TRAP. CD11b was counterstained with hematoxylin. Scale bars -50 μ m.



D

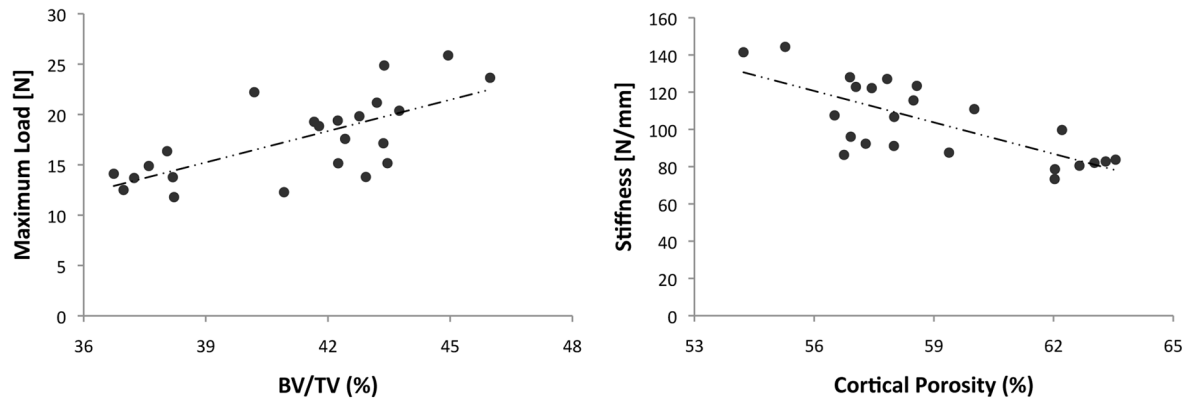
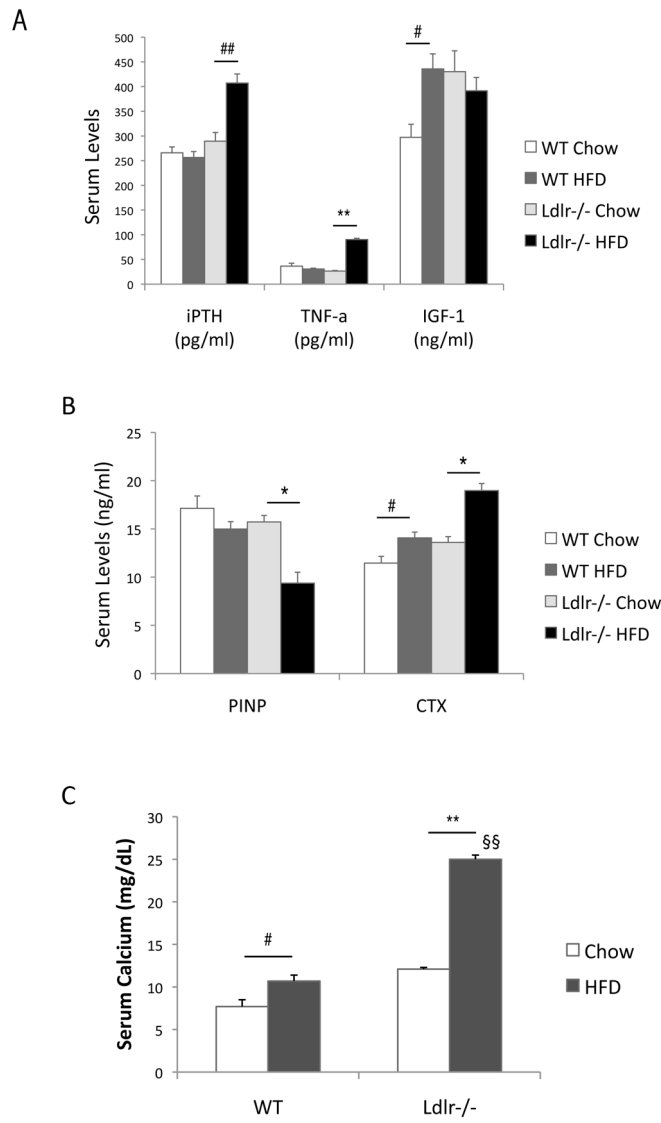


Figure 2. Effects of the HF diet on femoral bone

(A–B) MicroCT analysis of cortical bone volume (BV/TV, %), percent cortical porosity (%) of WT and *Ldlr*^{-/-} mice, with or without the HF diet (HFD), and/or D-4F. (C) Three-point bending analysis. (D) Correlation between microCT and mechanical parameters. ** $p < 0.0001$, * $p < 0.001$, # $p < 0.05$.



D

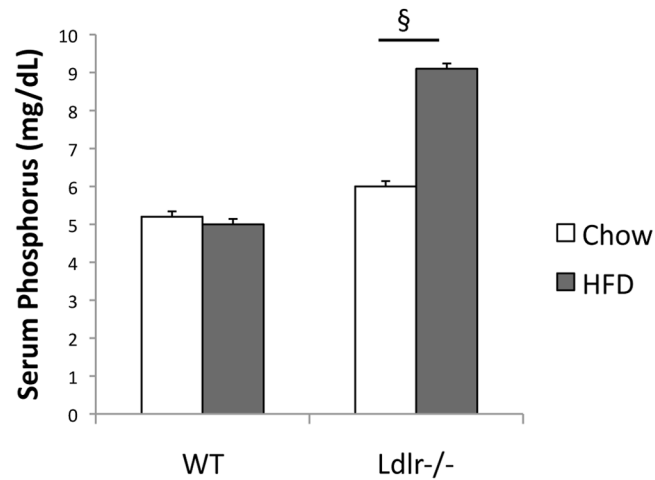


Figure 3. Effects of the HF diet on serum bone markers

ELISA of (A) intact PTH (iPTH), TNF- α and IGF-1, (B) bone formation marker, procollagen type I N-terminal propeptide (PINP) and bone resorption marker, type I collagen C-telopeptides (CTX), and (C) serum calcium (D) serum phosphorus. $**p < 0.0001$, $*p < 0.001$, $##p < 0.005$, $#p < 0.05$, $§§$ Possible pseudohypercalcemia. $§$ This difference greatly exceeds the known SD for this assay per manufacturer.

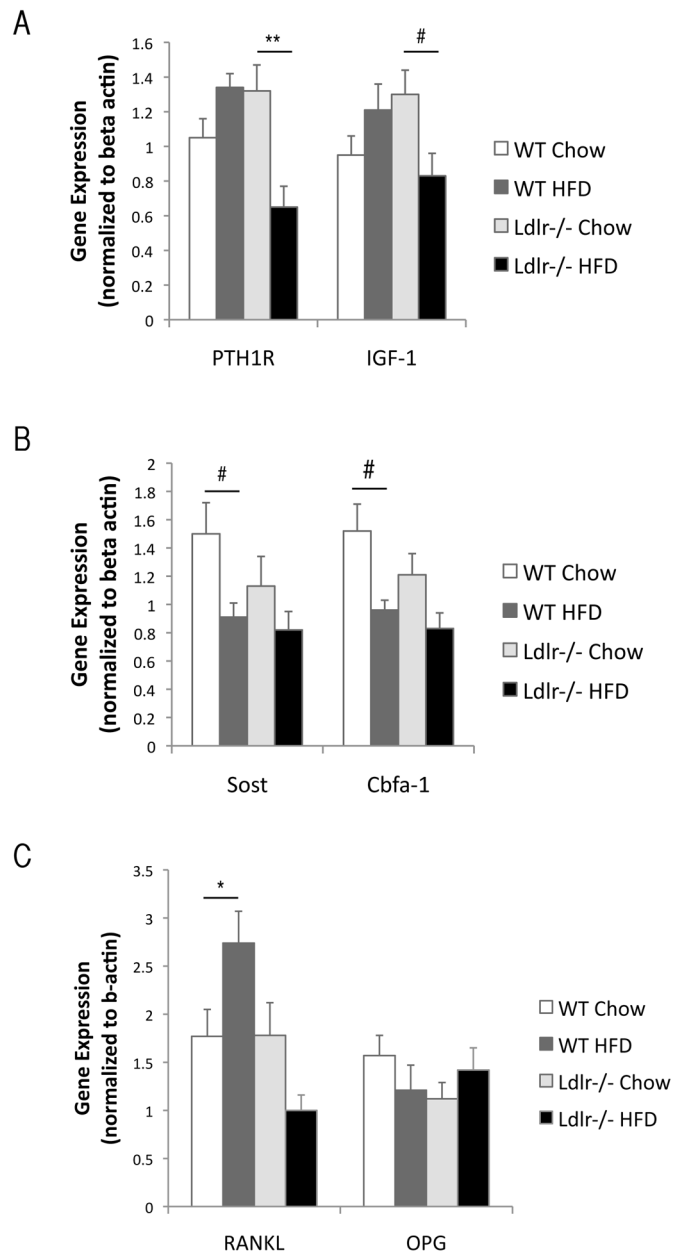


Figure 4. Effects of the HF diet on gene expression

Realtime RT-qPCR analysis of (A) PTH receptor (PTH1R), IGF-1, (B) Sclerostin (Sost), core binding factor a-1 (Cbfa-1), and (C) RANKL and osteoprotegerin (OPG) from humeri of WT and *Ldlr*^{-/-} mice, with or without the HF diet (HFD). ** $p < 0.01$, # $p < 0.05$, * $p = 0.05$.

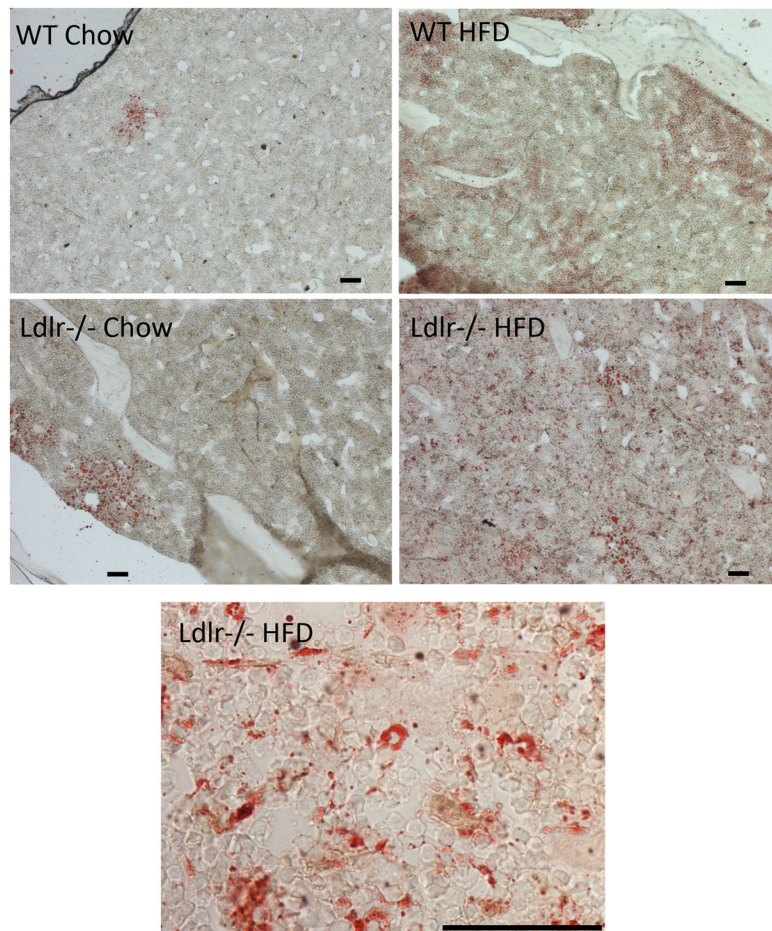


Figure 5. Effects of the HF diet on lipid accumulation

Oil red O stain of OCT embedded tibial bones from WT and *Ldlr*^{-/-} mice, with or without the HF diet (HFD). Scale bar -50 μ m.

Table I

Serum lipid and glucose levels

(mg/dL)	WT		<i>Ldlr</i> ^{-/-}	
	Chow	HFD	Chow	HFD
Triglycerides	35 ± 1	13 ± 0**	101 ± 1	75 ± 2**
Total Cholesterol	112 ± 1	283 ± 5**	380 ± 10	3085 ± 43**
HDL Cholesterol	88 ± 2	70 ± 1**	117 ± 3	7 ± 0**
Free Fatty Acids	24 ± 1	22 ± 0*	40 ± 1.0	49 ± 2*
Glucose	243 ± 5	234 ± 3	234 ± 7	397 ± 4**

* p < 0.005,

** p < 0.05 vs. respective Chow controls.

Table II

Trabecular histomorphometric parameters of femoral metaphysis

	WT		<i>Ldl</i> ^{-/-}	
	Chow	HFD	Chow	HFD
B. Ar (mm ²)	0.47 ± 0.04	0.35 ± 0.03**	0.45 ± 0.03	0.34 ± 0.02**
BV/TV (%)	12.49 ± 1.25	9.45 ± 0.92	11.94 ± 0.75	9.08 ± 0.46**
Tb.Th (μm)	34.43 ± 1.86	28.42 ± 1.44**	36.06 ± 1.53	26.98 ± 0.80*
BFR/BS (μm ³ /μm ² /y)	8.54 ± 1.47	30.67 ± 6.36**	15.18 ± 3.13	18.07 ± 4.83
MS/BS (%)	3.12 ± 0.54	8.56 ± 1.32**	5.22 ± 1.14	6.37 ± 1.37
Ob.S/BS (%)	3.66 ± 0.63	2.92 ± 0.92	2.50 ± 0.89	1.25 ± 0.30
Oc.S/BS (%)	2.23 ± 0.46	2.41 ± 0.56	1.99 ± 0.28	1.78 ± 0.36
N.Ob/T.Ar (mm ⁻²)	16.68 ± 2.68	13.03 ± 4.23	8.96 ± 2.86	5.11 ± 1.35
N.Oc/T.Ar (mm ⁻²)	4.75 ± 0.90	4.61 ± 0.94	3.98 ± 0.49	3.68 ± 0.71

B. Ar = bone area; BV = bone volume; TV = tissue volume; Tb.Th = trabecular thickness; BFR = bone-formation rate; MS = mineralizing surface; BS = bone surface; N.Ob = number of osteoblasts; N.Oc = number of osteoclasts; T.Ar = tissue area;

* p < 0.005,

** p < 0.05 vs. respective Chow controls.

Table III

Serum levels of bone resorption markers

(pg/dL)	WT		<i>Ldlr</i> ^{-/-}	
	Chow	HFD	Chow	HFD
RANKL	195 ± 11	163 ± 17	449 ± 14	200 ± 13**
OPG	456 ± 13	801 ± 12**	371 ± 4	776 ± 5**

** p < 0.0001 vs. respective Chow controls.